Available online at www.sciencedirect.com
ScienceDirect
International Journal of Mass Spectrometry 261 (2007) 25–31
International Journal of Mass Spectrometry
www.elsevier.com/locate/ijms

A new method of measuring neutral radicals by mass spectrometry

Zhaokui Wang [a,*], Yanhui Lou [a], Kuixun Lin [b], Xuanying Lin [b]

[a] College of Physics and Information Engineering, Henan Normal University, Xinxiang 453007, China
[b] Department of Physics, Shantou University, Shantou, Guangdong 515063, China

Received 6 June 2006; received in revised form 20 July 2006; accepted 21 July 2006
Available online 23 August 2006

Abstract

A new method, straight-line fitting, is proposed for measuring neutral radicals in plasma by a residual gas analyzer. Compared to threshold-ionization mass spectrometer, the proposed method is suited to all mass spectrometers, even if the minimum electron energy of the mass spectrometer is larger than the ionization threshold of the radicals. Moreover, the effects of the formation of daughter ions in the mass spectrometry ionization chamber are discussed. The results show that the effects of neutral radicals being ionized into fragment ions can be neglected during the course of deducing plasma depletion fraction within the deviation of the statistical fluctuation. In order to estimate the feasibility and reliability of this method, SiH_n ($n = 0$–3) radicals in an SiH_4 plasma and $SiCl_n$ ($n = 0$–2) radicals in an $SiCl_4$ plasma are measured. The experimental results demonstrate that this newly proposed method is universal and more accurate than the previous one.

Keywords: Straight-line fitting method; Mass spectrometry diagnosis; Neutral radical measurement; Daughter ions

1. Introduction

Plasma created by radio frequency (rf) glow discharges for chemical vapor deposition (CVD) process are widely used in the preparation of amorphous silicon (a-Si) and polycrystalline silicon (poly-Si) films due to their successful applications in various optoelectronic devices, such as thin film solar cells, thin film transistors, and switching devices [1–4]. The diagnosis and measurement of the primary particles in deposition and etching processes make it possible to understand the mechanism of film deposition and etching, which can improve the quality and photoelectric characteristics of films.

Both optical emission spectroscopy and broadband UV absorption spectroscopy are powerful plasma diagnostic techniques with high accuracy and spatial resolution. SiH_n ($n = 0$–3) and $SiCl_n$ ($n = 0$–2) concentrations in deposition and etching processes of films have been measured by them successfully in earlier studies [5–11]. However, both the absorption and emission spectra of these radicals generally cover a wide range, from the ultraviolet spectral region to the visible light spectral region. Consequently, all radicals in plasma cannot be measured by only one optical spectrometer. Mass spectroscopic analysis is a simple and useful technique for plasma diagnosis. It is superior to optical spectroscopic diagnosis in identification of plasma components and in the measurement of particle concentrations in plasma vapor and in the interaction between the plasma and surfaces, and it can measure simultaneously relevant species covering a large mass range. Mass spectrometry has been widely used for gas component identification and plasma analysis, particularly for detecting ions and neutral radicals. In previous studies, it was necessary to disperse the mass spectrometric signals at the different ionization thresholds of the neutral radicals [12–15], resulting in a significant measurement error.

In previous studies, the abundances of neutral radicals generated by plasmas have been measured using mass spectrometry [12,16,17]. In this paper, we give a new method to measure the radical abundance. First, we propose a straight-line fitting method to deduce the depletion fraction of the plasma by using the mass spectrometric signals of a residual gas analyzer (RGA). It is well known that the neutral radicals in the RGA ionization chamber will be ionized into both parent ions and fragment ions. Therefore, the effects of the formation of fragment ions need to be addressed. The feasibility and the reliability of a straight-line fitting method is evaluated. As examples, SiH_n ($n = 0$–3) radicals in an SiH_4 plasma and $SiCl_n$ ($n = 0$–2) radicals in an $SiCl_4$ plasma were measured.

* Corresponding author. Tel.: +86 373 3326151; fax: +86 373 3326151.
E-mail address: zhaokuiwang@163.com (Z.K. Wang).

1387-3806/$ – see front matter © 2006 Elsevier B.V. All rights reserved.
doi:10.1016/j.ijms.2006.07.012

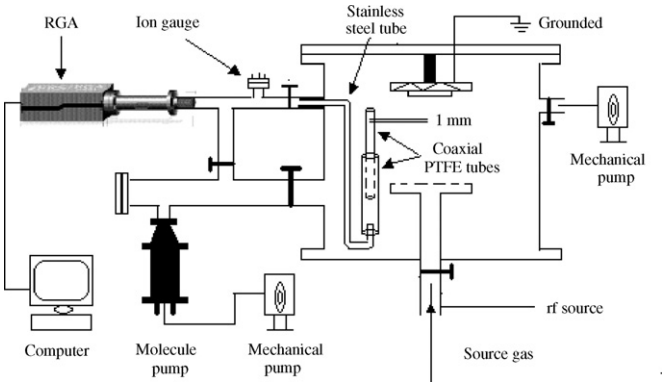

Fig. 1. Schematic of experimental apparatus for on-line mass spectroscopic analysis of neutral radicals in plasma.

2. Experimental arrangements

2.1. RGA and mass spectrometry sampling apparatus

The mass spectroscopy signals of the gas species from a plasma are detected by a residual gas analyzer (SRS RGA-100) with a minimum detectable partial pressure of 6.7×10^{-12} Pa. The SRS RGA is a mass spectrometer consisting of a quadrupole probe, and an electronics control unit (ECU) which mounts directly on the probe's flange, and contains all the electronics necessary to operate the instrument. The probe consists of three parts like other type mass spectrometers: the ionizer, the quadrupole filter and the ion detector. Positive ions are produced in the ionizer by bombarding gas molecules with electrons derived from a heated filament. The ions are then directed toward the entrance of the quadrupole mass analyzer where they are separated based on their mass-to-charge ratio. Ions that successfully pass through quadrupole are focused on the detector by an exit aperture held at ground potential. The detector measures the ion currents directly (Faraday cup) or, using an optional electron multiplier detector, measures an electron current that is proportional to the ion current. The ECU completely controls the operation of the RGA and handles and transmits its data to the computer for analysis and display. The instrument is operated by a RGA Windows software package that runs on IBM compatible PC's.

The mass spectrometry sampling apparatus is depicted in Fig. 1. A thin glass tube with an inner diameter of 1 mm is located between the plasma electrodes. One end of the glass tube is used as a sampling aperture on the central symmetry axis of the parallel electrodes. The other is inserted into the upper column of coaxial Teflon tubes. The bottom part of the column is linked to the RGA ionization chamber through a stainless steel tube with an inner diameter of 3 mm. The inner column and its outer tube consisting of the coaxial Teflon tube are well matched and the inner column can slide smoothly in the outer tube allowing the sampling position to be changed along the central symmetry axis from the bottom electrode to the upper electrode. Because the glass tube immersed in the plasma is so thin, disturbance of the discharge plasma is negligible.

2.2. Plasma enhanced chemical vapor deposition system

The discharge chamber is equipped with two parallel plate electrodes made of stainless steel. The glow discharge plasma in the chamber is generated by a capacitively coupled rf power source and confined in the space between the parallel electrodes with a gap of 30 mm for SiH_4 and $SiCl_4$ plasma. The flow rate of source gas is controlled by a mass flowmeter. The sampled gas species from the plasma region are leaked into the RGA ionization chamber via the above-mentioned movable gas sampling apparatus. Due to the fact that the filament of the RGA must be operated under a high vacuum environment, it is important for the differentially pumping system to keep the RGA ionization chamber at a stable pressure less than 10^{-2} Pa.

3. Computational methodology

3.1. Extrapolation of the plasma depletion fraction

In SiH_4 and $SiCl_4$ plasmas, there are electrons, ions, neutral radicals, SiH_4 and $SiCl_4$ molecules. Only the neutral radicals were sampled by mass spectrometry. The ions were removed by adding a suitable electromagnetic field at the sampling aperture. The mass spectroscopic signals with the plasma off, $S^n_{\text{off}}(E_e)$, and with it on, $S^n_{\text{on}}(E_e)$, were measured on the RGA, where E_e is the ionizing electron energy. S^n_{on}(Ee) can be generally written as

$$S^n_{\text{on}}(E_e) = S^n_{\text{ion}} + S^n(E_e) + (1-f)S^n_{\text{off}}(E_e), \quad (1)$$

where $S^n(E_e)$ is the mass spectroscopic signals of SiH_n and $SiCl_n$ radicals sampled from the glow discharge chamber, S^n_{ion} corresponds to signals of SiH_n^+ and $SiCl_n^+$ which were created in the discharge chamber and leaked into the RGA, and f is defined as the depletion fraction of the plasma.

In our experiments, with the RGA filament off, the leakage ion signals were too weak to be detected even if the RGA was set at maximum sensitivity, perhaps due to ion collisions with the wall of the gas sampling tube. Consequently, Eq. (1) reduces to

$$S^n_{\text{on}}(E_e) = S^n(E_e) + (1-f)S^n_{\text{off}}(E_e). \quad (2)$$

When the electron energy of the RGA was varied over the range of 50–100 eV, the contribution of $S^n(E_e)$ to $S^n_{\text{on}}(E_e)$ was negligible and the ratio of $S^n_{\text{on}}(E_e)/S^n_{\text{off}}(E_e)$ was almost a constant regardless of the rf power and the discharge pressure. Eq. (2) then reduces to

$$S^n_{\text{on}}(E_e) = (1-f)S^n_{\text{off}}(E_e). \quad (3)$$

This gave us a simple method to obtain the plasma depletion fraction by the following equation at high electron energy:

$$f = \frac{S^n_{\text{off}}(E_e) - S^n_{\text{on}}(E_e)}{S^n_{\text{off}}(E_e)}. \quad (4)$$

Robertson et al. had measured the depletion faction of the SiH_4 plasma by this method [12,16,17].

Table 1
The ionization cross-sections $\sigma_n(E_e)$ of $SiCl_n$ ($n = 1$ and 2) radicals (10^{-16} cm^2)

Electron energy (eV)	Ionization cross-section (in 10^{-16} cm^2)	
	SiCl (IP[a]: 10.93 eV)	$SiCl_2$ (IP[a]: 10.93 eV)
15	0.33	0.46
20	1.63	1.88
25	2.74	3.59
30	3.54	5.06
35	4.19	5.99
40	4.66	6.76
45	5.03	7.54
50	5.36	8.13
60	5.82	9.03
70	6.14	9.59
80	6.37	9.86
90	6.52	10.08
100	6.63	10.22

[a] Assumed ionization potential (IP).

Although the plasma depletion fraction is a constant under certain discharge conditions and sampling position, all the intensities of $S^n_{off}(E_e)$, $S^n_{on}(E_e)$ and $S^n(E_e)$ are changing with the electron energy of the RGA because the ionization cross-sections of the neutral radicals are functions of electron energy. Hence Eq. (2) becomes:

$$S^n_{on}(E_e) = \alpha_n(E_e)S^n_0 + (1 - f)S^n_{off}(E_e), \quad (5)$$

where $\alpha_n(E_e)$ is defined as

$$\alpha_n(E_e) = \frac{\sigma_n(E_e)}{\sigma_{n\,max}(E^n_{em})}, \quad (6)$$

$\sigma_n(E_e)$ and $\sigma_{n\,max}(E^n_{em})$ are the ionization cross-sections at electron energy (E_e) and the maximum ionization cross-section corresponding to the electron energy (E^n_{em}) for SiH_n and $SiCl_n$ radicals. The values of $\sigma_n(E_e)$ of SiH_n radicals are cited from the data of Ref. [18], the values of $\sigma_n(E_e)$ of $SiCl_n$ radicals are calculated using the theoretical models and calculation method of Joshipura [19] and expressed in Table 1. S^n_o is defined as the mass spectroscopic signal of SiH_n and $SiCl_n$ at electron energy E^n_{em} corresponding to the maximum ionization cross-section.

Eq. (5) can be simplified to

$$C^n_1 = -S^n_0 + fC^n_2, \quad (7)$$

where, $C^n_1 = (S^n_{off}(E_e) - S^n_{on}(E_e))/\alpha_n(E_e)$ and $C^n_2 = S^n_{off}(E_e)/\alpha_n(E_e)$. The values of C^n_1 and C^n_2 can be calculated over the whole electron energy range of RGA. According to Eq. (7), we propose a straight-line fitting of C^n_1 and C^n_2 corresponding to the whole electron energy (>25 eV) range of RGA. The slope of the line is f. Due to the smaller mass range of RGA-100 only the SiH_n^+ ($n = 0$–4) signals and only the $SiCl_n^+$ ($n = 0$–2) signals were detected by it. In our experiments, the depletion fraction of the SiH_4 plasma was deduced by the continued SiH, SiH_2 and SiH_3 mass spectrometric signals and the depletion fraction of the $SiCl_4$ plasma by the SiCl and $SiCl_2$ mass spectrometric signals.

Since C^n_1 versus C^n_2 were obtained over the whole electron energy ranges of the mass spectrometer, the new method is universal compared with the existing one that is applicable only at high electron energy. Because the contribution of $S_n(E_e)$ to $S^n_{on}(E_e)$ was not neglected, the new method should be more accurate than the existing one.

3.2. Effects of the formation of daughter ions in the RGA ionizer

For a given target radicals impacted by electron there exists a parent ionization process and a dissociative ionization process. The neutral radicals will ionized into corresponding parent ions and fragment ions by electrons emitted from the filament. Although the dissociative ionization cross-sections of the radicals are smaller than the ionization cross-sections of the radicals, they have the same magnitude.

Take the SiH_4 plasma as an example. SiH_3 radicals are ionized into SiH_3^+ and dissociatively ionized into SiH_2^+. Analogously, SiH_2 radicals are ionized into SiH_2^+ and dissociatively ionized into SiH^+, SiH radicals ionized into SiH^+ and dissociatively ionized into Si^+. Generally, both the ionization cross-section and the dissociative ionization cross-section of SiH_n are functions of electron energy. Hence, another parameter $\beta_n(E_e)$ should be introduced in the course of deducing the plasma depletion fraction:

$$\beta_n(E_e) = \frac{\sigma_n(E_e)}{\sigma_n(E_e) + \sigma_{n'}(E_e)}, \quad (8)$$

where, $\sigma_{n'}(E_e)$ is the dissociative ionization cross-section of SiH_n at the electron energy E_e.

Thus, for SiH_3, $S^3_{on}(E_e)$ can be expressed as follows:

$$S^3_{on}(E_e) = S^3_0\alpha_3(E_e)\beta_3(E_e) + (1 - f)S^3_{off}(E_e) \quad (9)$$

In the right of Eq. (9), the first and second terms are the contribution of SiH_3 radicals and SiH_4 molecules sampled from the SiH_4 plasma on the SiH_3^+ mass spectrometric signals, respectively.

Analogously, for SiH_2 and SiH, $S^2_{on}(E_e)$ and $S^1_{on}(E_e)$ can be expressed as Eqs. (10) and (11), respectively,

$$S^2_{on}(E_e) = S^2_0\alpha_2(E_e)\beta_2(E_e) + S^3_0\alpha_3(E_e)(1 - \beta_3(E_e)) + (1 - f)S^2_{off}(E_e) \quad (10)$$

$$S^1_{on}(E_e) = S^1_0\alpha_1(E_e)\beta_1(E_e) + S^2_0\alpha_2(E_e)(1 - \beta_2(E_e)) + (1 - f)S^1_{off}(E_e) \quad (11)$$

In the right of Eq. (10), the first and third terms are the contributions of SiH_2 radicals and SiH_4 molecules sampled from the SiH_4 plasma on SiH_2^+ mass spectrometric signals, respectively, and the second term is the contribution of SiH_3 radicals being dissociative ionized into SiH_2^+ ions.

In the right of Eq. (11), the first and third terms are the contributions of SiH radicals and SiH_4 molecules on SiH^+ and the second term is the contribution of SiH_2 radicals being dissociatively ionized into SiH^+ ions.

Table 2
The values of $\alpha_n(E_e)$ and $\beta_n(E_e)$ for SiH_n ($n = 1$–3) radicals

E_e (eV)	α_1	α_2	α_3	β_1	β_2	β_3
25	0.6946	0.5400	0.5530	0.8107	0.7068	0.7413
30	0.7459	0.6907	0.7280	0.7688	0.7175	0.7424
40	0.8459	0.7867	0.8560	0.7417	0.7248	0.7572
50	0.9459	0.8827	0.9348	0.7479	0.7356	0.7594
60	0.9892	0.9680	0.9783	0.7500	0.7469	0.7643
70	1.0000	1.0000	1.0000	0.7475	0.7470	0.7651
80	1.0000	0.9973	0.9918	0.7490	0.7480	0.7636
90	0.9811	0.9920	0.9864	0.7485	0.7516	0.7642
100	0.9622	0.9760	0.9755	0.7479	0.7531	0.7671

Furthermore, Eqs. (9)–(11) can be simplified as the following forms:

$$C_1^3 = -S_0^3 + fC_2^3 \tag{12}$$

$$C_1^2 = -S_0^2 + fC_2^2 \tag{13}$$

$$C_1^1 = -S_0^1 + fC_2^1 \tag{14}$$

where

$$C_1^3 = \frac{S_{off}^3(E_e) - S_{on}^3(E_e)}{\alpha_3(E_e)\beta_3(E_e)}, \qquad C_2^3 = \frac{S_{off}^3(E_e)}{\alpha_3(E_e)\beta_3(E_e)} \tag{15}$$

$$C_1^2 = \frac{(1-\beta_3(E_e))\alpha_3(E_e)S_0^3 + S_{off}^2(E_e) - S_{on}^2(E_e)}{\alpha_2(E_e)\beta_2(E_e)},$$

$$C_2^2 = \frac{S_{off}^2(E_e)}{\alpha_2(E_e)\beta_2(E_e)} \tag{16}$$

$$C_1^1 = \frac{(1-\beta_2(E_e))\alpha_2(E_e)S_0^2 + S_{off}^1(E_e) - S_{on}^1(E_e)}{\alpha_1(E_e)\beta_1(E_e)},$$

$$C_2^1 = \frac{S_{off}^1(E_e)}{\alpha_1(E_e)\beta_1(E_e)} \tag{17}$$

In Eq. (15)–(17), $S_{off}^n(E_e)$ and $S_{on}^n(E_e)$ of SiH_n ($n = 0$–3) radicals are measured by the residual gas analyzer, the values of $\alpha_n(E_e)$ and $\beta_n(E_e)$ are calculated through Eqs. (6) and (8) and collected in Table 2. The ionization and dissociative ionization cross-sections of SiH_n ($n = 1$–3) radicals are cited in Refs. [18].

Using Eq. (12), we carry out a linear fit on C_1^3 versus C_2^3 corresponding to the whole electron energy range of the mass spectrometer. The slope of the line yields f. Simultaneously, the value of S_0^3 can be obtained from the intercept.

In the same way, using Eqs. (13) and (14), we obtain the SiH_4 depletion fraction which is deduced from the SiH_2 and SiH mass spectrometric signals. In the course of deduction, S_0^3 and S_0^2 is derived from Eqs. (12) and (13), respectively.

Fig. 2 shows the curves of SiH_4 depletion fraction (deduced by linear fitting method and revised linear fitting method, respectively) versus sampling position at chamber pressure $P = 10$ Pa and rf power $P_{rf} = 10$ W. In most sampling positions, the values of the depletion fraction deduced are close except that there is a maximum discrepancy 9% at a position 15 mm away from the cathode.

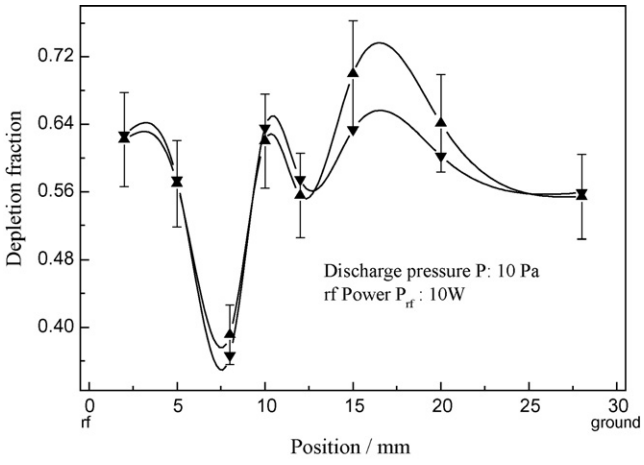

Fig. 2. The comparison of SiH_4 depletion fractions deduced by linear fitting method and revised linear fitting method (▲, by linear fitting method; ▼, by revised linear fitting method).

It is known that parent ionization is the dominant process and the most prominent dissociative ionization channel is the one in which one H atom is removed, i.e., $SiH_n \rightarrow SiH_{n-1}^+ + H$. From Ref. [19], we can see that the dissociative ionization cross-section is generally a quarter of the parent ionization cross-section of SiH_n ($n = 1$–3). If the SiH_n densities in the mass spectrometer have the same magnitude, the mass spectrometric signal

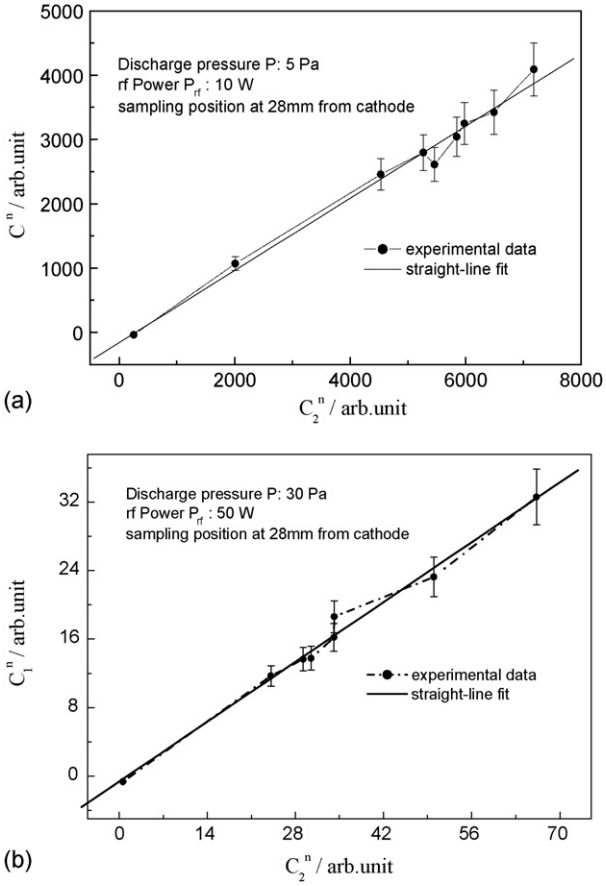

Fig. 3. The graphs of straight-line fit of C_1^n vs. C_2^n corresponding to SiH_2 for (a) and SiCl for (b).

intensities of SiH_n^+ should be close no matter what. The SiH_n densities in the plasma usually have the same magnitude as has been verified by our previous experimental measurement [20].

In all, the effects of the formation of daughter ions can be neglected only of the radical concentrations in the plasma have the same magnitude.

3.3. Feasibility and reliability of the extrapolation method

From Eq. (7), it is obvious that C_1^n is a simple function of C_2^n and there should be a good linear relation between the values of C_1^n and C_2^n. We calculated many groups values of C_1^n and C_2^n using $S_{\text{off}}^n(E_e)$ and $S_{\text{on}}^n(E_e)$ mass spectrometric signals of neutral radicals. Fig. 3(a) and (b) show the straight-line fit of C_1^n and C_2^n corresponding to SiH_2 and SiCl. In Fig. 3(a), there is 10% maximum error between the value of C_2^n calculated from the SiH_2 mass spectrometric signal and the value deduced by linear fit at E_e 60 eV. In Fig. 3(b), the values of C_2^n calculated from the SiCl mass spectrometric signals are generally in good agreement with that deduced by the linear fit except that there is 9% maximum error at the E_e 70 eV. A good linear relation of C_1^n and C_2^n demonstrates that the straight-line fitting method to deduce the depletion fraction of the plasma is feasible.

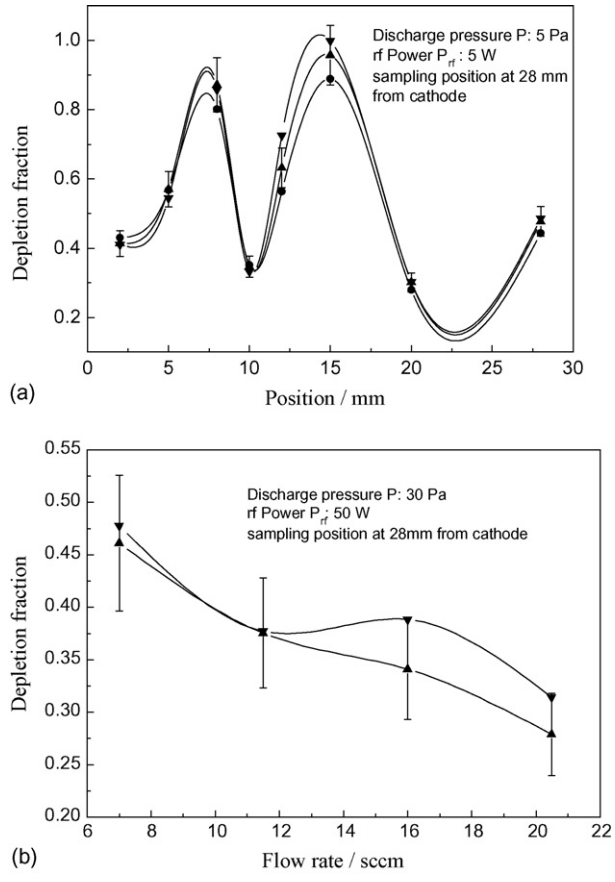

Fig. 4. (a) Depletion fractions of SiH_4 deduced by SiH, SiH_2 and SiH_3 mass spectrometric signals (▲, by SiH mass spectrometric signal; ▼, by SiH_2 mass spectrometric signal; ●, by SiH_3 mass spectrometric signal). (b) Depletion fractions of $SiCl_4$ deduced by SiCl and $SiCl_2$ mass spectrometric signals (▲, by SiCl mass spectrometric signal; ▼, by $SiCl_2$ mass spectrometric signal).

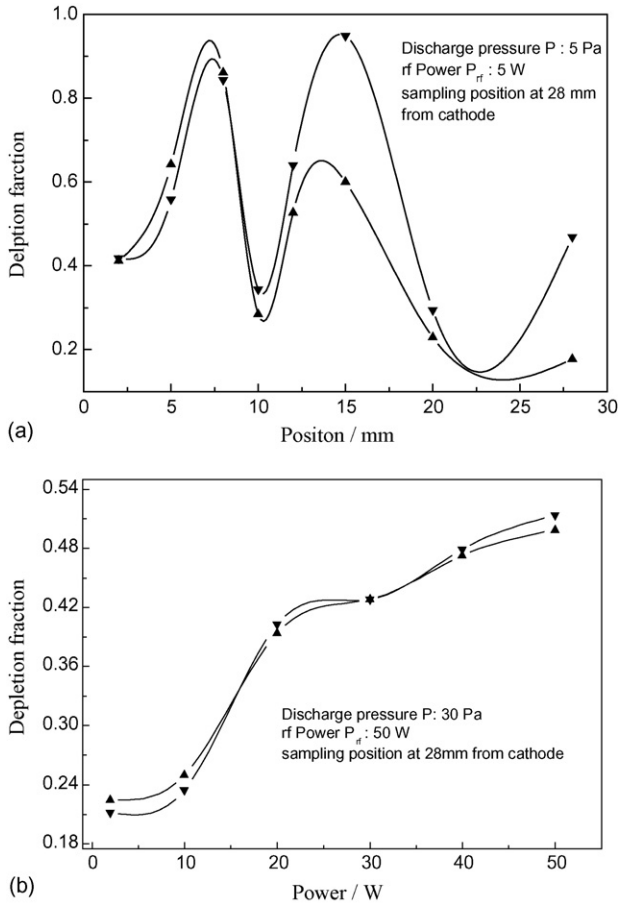

Fig. 5. (a) Depletion fractions of SiH_4 deduced by the new method and the existing one (▲, f' by the previous method; –▼, f by the straight-line fitting method). (b) Depletion fractions of $SiCl_4$ deduced by the new method and the existing one (▲, f' by the previous method; ▼, f by the straight-line fitting method).

Theoretically speaking, the depletion fraction of the plasma should be a constant no matter which neutral radical mass spectrometric signal is used to deduce it. Fig. 4(a) shows the curves of SiH_4 depletion fraction f (deduced from the SiH, SiH_2, and SiH_3 mass spectrometric signals, respectively) versus position z, and Fig. 4(b) shows the curves of $SiCl_4$ depletion fraction f (deduced from the SiCl and $SiCl_2$ mass spectrometric signals) versus flow rate. It is obvious that although the plasma depletion fractions are deduced by different neutral radical mass spectroscopic signals, they are very close and within the deviation of the statistical fluctuations.

Fig. 5(a) shows the SiH_4 depletion fraction versus sampling position deduced by the new method and by the existing one, and Fig. 5(b) shows the $SiCl_4$ depletion fraction versus rf power deduced by two methods.

From Fig. 5(a) and (b), we can see that the plasma depletion f (by the straight-line fitting method) and f' (by the previous method) are almost equal, and f is slightly larger than f' under the same experimental conditions. f is obtained using the following equation which is directly derived analogous to Eq. (4):

$$f = \frac{S_{\text{off}}^n(E_e) - S_{\text{on}}^n(E_e) + S^n(E_e)}{S_{\text{off}}^n(E_e)}. \quad (18)$$

The contribution of $S^n(E_e)$ on $S^n_{on}(E_e)$ is not neglected in Eq. (18). Comparing Eqs. (4) and (18), f is larger than f' naturally. This demonstrates that the new method is more accurate than the existing one.

In a word, a good linear relation of the extrapolation formula of the plasma depletion fraction was verified by the experimental results, the straight-line fit method is feasible and reliable to deduce the plasma depletion fraction. The proposed new method of measuring plasma depletion fraction is universal and more accurate than the existing one.

4. Spatial distributions of neutral radicals

Define $S^n(E_{e0})$ as the S^n value at electron energy E_{e0}. Then, $S^n(E_{e0})$ can be given as following:

$$S^n(E_{e0}) = S^n_{on}(E_{e0}) - (1 - f)S^n_{off}(E_{e0}). \quad (19)$$

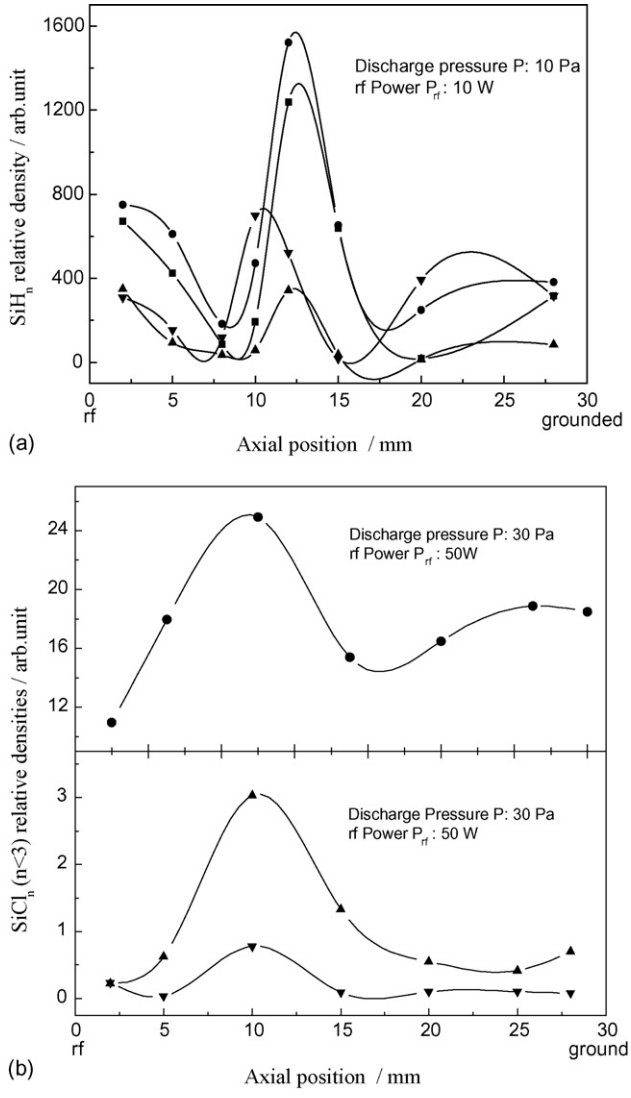

Fig. 6. (a) The axial distribution of SiH_n ($n = 0$–3) relative densities in SiH_4 plasma (■, for SiH_3; ●, for SiH_2; ▲, for SiH; ▼, for Si). (b) The axial distribution of $SiCl_n$ ($n < 3$) relative densities in $SiCl_4$ plasma (●, for Si; ▲, for SiCl; ▼, for $SiCl_2$).

Obviously, $S^n(E_{e0})$ characterizes the abundances of neutral radicals in the plasma.

Utilizing Eq. (19), at $E_{e0} = 40$ eV, we calculate the abundances of the SiH_n ($n = 0$–3) and $SiCl_n$ ($n = 0$–2) radicals under different experimental conditions. Fig. 6(a) and (b) show the axial orientation distribution of SiH_n ($n = 0$–3) and $SiCl_n$ ($n = 0$–2) abundances, respectively.

From Fig. 6(a), we can see that there are abundance peaks at position 13 mm (near the middle of two parallel electrodes) for SiH, SiH_2 and SiH_3 and at 10 mm for Si. Generally, in a silane plasma, SiH_2 and SiH_3 are the dominant species among the SiH_n ($n = 0$–3) radicals, Si is secondary, and SiH is the least abundant radical. This suggests that SiH_2 and SiH_3 are the major primary species forming the amorphous silicon film.

From Fig. 6(b), it is obvious that the abundances of the $SiCl_n$ ($n = 0$–2) radicals have peak values 10 mm away from the rf powered electrode along the axial orientation. And we can see that Si is the most abundant radical in a $SiCl_4$ plasma, SiCl is next, and $SiCl_2$ is less than SiCl. Hence Si and SiCl are the dominant precursors in forming the polycrystalline silicon film.

These measured spatial distributions of SiH_n ($n = 0$–3) and $SiCl_n$ ($n = 0$–2) radicals can provide useful data for researching the plasma spatial reaction process and understanding the deposition and etching mechanism of thin films. Moreover, further research on the spatial distribution of SiH_n ($n = 0$–3) and $SiCl_n$ ($n = 0$–2) radicals is useful for improving the quality and photoelectric properties of thin films.

5. Conclusions

The paper proposes a new method, straight-line fitting, to deduce the plasma depletion fraction by a residual gas analyzer. The effects of the formation of daughter ions is minimized, and the experimental data demonstrate that the parent ionization process dominates if the various radical concentrations in the plasma have the same magnitude. The new method is suitable for all mass spectrometers even if the minimum electron energy is larger than the ionization thresholds of radicals formed. What is more, the new method is feasible, reliable, and the newly proposed method is universal and more accurate than the existing one. Finally, utilizing the depletion fraction of the plasma, we measure the spatial distributions of SiH_n ($n = 0$–3) in a SiH_4 plasma and $SiCl_n$ ($n = 0$–2) radicals in a $SiCl_4$ plasma. The information is beneficial to researching the spatial reaction process in plasma and understanding the deposition mechanism of thin films.

Acknowledgements

The authors gratefully acknowledge Prof. K.N. Joshipura for calculating the ionization cross-sections $\sigma_n(E_e)$ of $SiCl_n$ ($n = 1$ and 2) radicals. This work has been supported by the National Key Basic Research Special Foundation of China under Grant No. G2000028208.

References

[1] S.D. Brotherton, C. Glasse, C. Glaister, P. Green, F. Rohlfing, J.R. Ayres, Appl. Phys. Lett. 84 (2004) 293.
[2] H. Sukti, R. Swati, Solid State commun. 109 (1998) 125.
[3] R. Dewarrat, J. Robertson, Appl. Phys. Lett. 82 (2003) 883.
[4] S. Sriraman, E.S. Aydil, D. Maroudas, J. Appl. Phys. 92 (2002) 842.
[5] T. Kunihide, M. Takuya, H. Hiroshi, Jpn. J. Appl. Phys. 30 (1991) L1208.
[6] K. Akihiro, K. Naoki, O. Kenichi, G. Toshio, Jpn. J. Appl. Phys. 32 (1993) L543.
[7] N. Yoshitaka, K. Koichi, M. Toshihiko, M. Kitazoe, K. Horii, H. Umemoto, A. Masuda, H. Matsumura, J. Appl. Phys. 88 (2000) 5437.
[8] R.S. Sansa, A.M. Ronn, Chem. Phys. 96 (1985) 183.
[9] N. Washida, Y. Matsumi, T. Hayashi, T. Ibuki, A. Hiraya, K. Shobatake, J. Chem. Phys. 83 (1985) 2769.
[10] J.O'. Neill, J. Singh, J. Appl. Phys. 76 (1994) 5967.
[11] J.P. Booth, G. Cunge, F. Neuilly, N. Sadeghi, Plasma Sources Sci. Technol. 7 (1998) 423.
[12] Robertson, A. Gallagher, J. Appl. Phys. 59 (1986) 3402.
[13] C. Murray, B. Wernsman, J. Appl. Phys. 72 (1992) 4556.
[14] M. Hertl, J. Jolly, J. Phys. D: Appl. Phys. 33 (2000) 381.
[15] A.M. Myers, D.N. Ruzic, R.C. Powell, N. Maley, D.W. Pratt, J.E. Greene, J.R. Abelson, J. Vac. Sci. Technol. A 8 (1990) 1668.
[16] K.X. Lin, X.Y. Lin, Z. Xu, Y.P. Yu, Mater. Res. Symp. Proc. 297 (1993) 37.
[17] K.X. Lin, X.Y. Lin, X. Zeng, Y.P. Yu, W.S. Deng, Chin. Phys. Lett. 10 (1993) 342.
[18] V. Tamovsky, H. Deutsch, K. Becker, J. Chem. Phys. 105 (1996) 6315.
[19] K.N. Joshipura, V. Minaxi, C.G. Limbachiya, B.K. Antony, Phys. Rev. A 69 (2004) 227051.
[20] Z.K. Wang, K.X. Lin, X.Y. Lin, G.M. Qiu, Z.S. Zhu, Chin. Phys. Lett. 4 (2005) 904.